Article

Multiple-Site Exchange in Proteins Studied with a Suite of Six NMR Relaxation Dispersion Experiments: An Application to the Folding of a Fyn SH3 Domain Mutant

Dmitry M. Korzhnev, Philipp Neudecker, Anthony Mittermaier, Vladislav Yu. Orekhov, and Lewis E. Kay

J. Am. Chem. Soc., **2005**, 127 (44), 15602-15611• DOI: 10.1021/ja054550e • Publication Date (Web): 12 October 2005

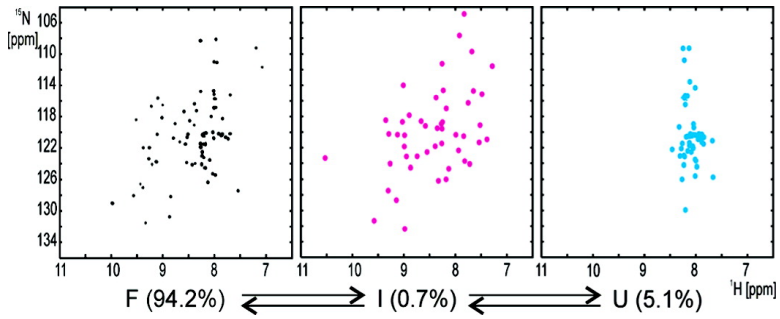

More About This Article

Additional resources and features associated with this article are available within the HTML version:

- Supporting Information
- Links to the 12 articles that cite this article, as of the time of this article download
- Access to high resolution figures
- Links to articles and content related to this article
- Copyright permission to reproduce figures and/or text from this article

View the Full Text HTML

J|A|C|S
ARTICLES
Published on Web 10/12/2005

Multiple-Site Exchange in Proteins Studied with a Suite of Six NMR Relaxation Dispersion Experiments: An Application to the Folding of a Fyn SH3 Domain Mutant

Dmitry M. Korzhnev,[†] Philipp Neudecker,[†] Anthony Mittermaier,[†] Vladislav Yu. Orekhov,[‡] and Lewis E. Kay*,[†]

Contribution from the Departments of Medical Genetics, Biochemistry, and Chemistry, The University of Toronto, Toronto, Ontario M5S 1A8, Canada, and Swedish NMR Center at Göteborg University, Box 465, 405 30 Göteborg, Sweden

Received July 8, 2005; E-mail: kay@pound.med.utoronto.ca

Abstract: The three-site exchange folding reaction of an ^{15}N-labeled, highly deuterated Gly48Met mutant of the Fyn SH3 domain has been characterized at 25 °C using a suite of six CPMG-type relaxation dispersion experiments that measure exchange contributions to backbone ^{1}H and ^{15}N transverse relaxation rates in proteins. It is shown that this suite of experiments allows the extraction of all the parameters of this multisite exchange process in a robust manner, including chemical shift differences between exchanging states, from a data set recorded at only a single temperature. The populations of the exchanging folded, intermediate, and unfolded states that are fit are 94, 0.7, and 5%, respectively. Despite the small fraction of the intermediate, structural information is obtained for this state that is consistent with the picture of SH3 domain folding that has emerged from other studies. Taken together, the six dispersion experiments facilitate the complete reconstruction of ^{1}H−^{15}N correlation spectra for the unfolded and intermediate states that are "invisible" in even the most sensitive of NMR experiments.

1. Introduction

Many biological processes, including enzyme catalysis[1] and molecular recognition,[2] involve conformational rearrangements that occur on a micro- to millisecond time scale. NMR relaxation dispersion techniques such as Carr−Purcell−Meiboom−Gill (CPMG)-type[3,4] and rotating-frame relaxation ($R_{1\rho}$)[5,6] experiments are powerful probes for the study of such dynamics. In the past few years, there have been significant advances in the development of relaxation dispersion methods.[6,7] For example, the existing ^{1}H and ^{15}N single-quantum (SQ) CPMG dispersion schemes that quantify microsecond−millisecond dynamics at backbone amide positions of proteins[8−10] have been supplemented by complementary experiments that measure relaxation dispersion of ^{1}H−^{15}N zero- (ZQ) and double- (DQ) quantum coherences[11,12] and by experiments that operate on multiple-quantum (MQ, equal sums of ZQ and DQ) coherences,[13] where trains of either ^{1}H or ^{15}N refocusing pulses are applied. It is thus possible to record a suite of six dispersion profiles for each backbone amide site, providing the opportunity to characterize exchange dynamics in some detail.

The extraction of accurate kinetic parameters that characterize a multi- (>two) site exchange process from relaxation dispersion data remains, however, a major challenge. In most studies of proteins published to date using this technique, the data have been analyzed under the assumption of two-site exchange. Although in some cases the two-site exchange model is justified,[14] in many cases of interest the dynamics are likely to be more complex. For example, ^{15}N dispersion studies of isomerization of disulfide linkages in BPTI showed clearly that the process involves a third state,[15] and similar experiments quantifying the folding kinetics of the drkN SH3 domain could only be interpreted in terms of a pair of exchange processes with rates that differed by more than 1 order of magnitude.[9] Enzyme function can often be described as a series of several (more than two) sequential steps, even for simple reactions, such as the one catalyzed by the peptidyl/prolyl isomerase cyclophilin A.[16] Multiple exchanging conformations of a peptide−protein

[†] University of Toronto.
[‡] Swedish NMR Center at Göteborg University.

(1) Fersht, A. *Structure and Mechanism in Protein Science*; W. H. Freeman and Company: New York, 1999.
(2) Pawson, T. *Nature* **1995**, *373*, 573−580.
(3) Carr, H. Y.; Purcell, E. M. *Phys. Rev.* **1954**, *4*, 630−638.
(4) Meiboom, S.; Gill, D. *Rev. Sci. Instrum.* **1958**, *29*, 688−691.
(5) Deverell, C.; Morgan, R. E.; Strange, J. H. *Mol. Phys.* **1970**, *18*, 553−559.
(6) Palmer, A. G.; Kroenke, C. D.; Loria, J. P. *Methods Enzymol.* **2001**, *339*, 204−238.
(7) Palmer, A. G., III; Grey, M. J.; Wang, C. *Methods Enzymol.* **2005**, *394*, 430−465.
(8) Loria, J. P.; Rance, M.; Palmer, A. G. *J. Am. Chem. Soc.* **1999**, *121*, 2331−2332.
(9) Tollinger, M.; Skrynnikov, N. R.; Mulder, F. A. A.; Forman-Kay, J. D.; Kay, L. E. *J. Am. Chem. Soc.* **2001**, *123*, 11341−11352.
(10) Ishima, R.; Torchia, D. *J. Biomol. NMR* **2003**, *25*, 243−248.
(11) Orekhov, V. Y.; Korzhnev, D. M.; Kay, L. E. *J. Am. Chem. Soc.* **2004**, *126*, 1886−1891.
(12) Dittmer, J.; Bodenhausen, G. *J. Am. Chem. Soc.* **2004**, *126*, 1314−1315.
(13) Korzhnev, D. M.; Kloiber, K.; Kay, L. E. *J. Am. Chem. Soc.* **2004**, *126*, 7320−7329.
(14) Choy, W. Y.; Zhou, Z.; Bai, Y.; Kay, L. E. *J. Am. Chem. Soc.* **2005**, *127*, 5066−5072.
(15) Grey, M. J.; Wang, C. Y.; Palmer, A. G. *J. Am. Chem. Soc.* **2003**, *125*, 14324−14335.
(16) Eisenmesser, E. Z.; Bosco, D. A.; Akke, M.; Kern, D. *Science* **2002**, *295*, 1520−1523.

10.1021/ja054550e CCC: $30.25

complex have been reported in an ^{15}N relaxation dispersion study of human prothrombin interacting with an antithrombic peptide.[17] In recent work from our laboratory, low populated folding intermediates along the (assumed) three-step folding trajectories of a pair of destabilized mutants of the Fyn SH3 domain have been characterized using ^{15}N SQ CPMG experiments.[18]

In "favorable" cases of multisite exchange, where the kinetics of each exchange process differ by at least 1 order of magnitude, it may be possible to extract the exchange parameters from fits of ^{15}N SQ data derived from a single residue.[15] Often, however, kinetic parameters are more similar and fits must rely on data recorded for multiple sites that are interpreted in the context of a global exchange model. Even in cases where ^{15}N SQ dispersion profiles for many residues can be fit simultaneously, it is not uncommon to obtain multiple solutions that fit the data (nearly) equally well. In such cases it is necessary to record data over a range of experimental conditions, such as temperature or substrate concentrations (in the case of binding reactions), to ensure that a true χ^2 minimum in solution space is found. For example, in the case of our studies of the folding of the Gly48Met and Gly48Val mutants of the Fyn SH3 domain, ^{15}N SQ dispersion data were collected at multiple temperatures, and three-site exchange parameters were obtained assuming (i) that the temperature dependence of exchange rate constants could be described by transition state theory and (ii) that ^{15}N chemical shift differences between the exchanging states, $\Delta\varpi_N$, are independent of temperature.[18] In studies of the human prothrombin/antithrombic peptide system, ^{15}N SQ dispersion measurements were performed at different molar ratios of protein and peptide, and the data were analyzed using three-site exchange models taking into account the concentration dependence of the exchange rate constants.[17]

The analysis of multisite exchange processes is significantly more complex than that for two-site exchanging systems, and it is clearly advantageous, therefore, to record as much complementary data as possible. Here we analyze a data set based on a suite of six ^{1}H$-^{15}$N CPMG-type dispersion experiments (recorded on an ^{15}N-labeled perdeuterated sample) that use backbone amide groups as probes to study the equilibrium folding/unfolding reaction of the Gly48Met Fyn SH3 domain that proceeds through the formation of a low populated intermediate state. Since all of the dispersion data are sensitive to the same set of exchange parameters (i.e., the same exchange rate constants and chemical shift differences between the exchanging states for both nuclei of the ^{1}H$-^{15}$N spin pair, $\Delta\varpi_H$ and $\Delta\varpi_N$), the combined use of six types of dispersion profiles provides distinct advantages over the analysis of SQ ^{15}N and ^{1}H data. Simulations that will be presented elsewhere establish, not surprisingly, that the addition of data, without the introduction of further adjustable exchange parameters, leads to a significant improvement in the precision of extracted parameters and in the convergence of the optimization protocol. We show, here, through both experiment and computations, that robust three-site exchange parameters characterizing the reaction F $\leftrightarrow$ I $\leftrightarrow$ U between a highly populated folded state (F) and two minor states, intermediate (I) and unfolded (U), can be obtained on the basis of a dataset measured at a *single* temperature. In contrast, a data set comprising a number of temperatures was necessary for the analysis of ^{15}N SQ data (exclusively) recorded on a fully protonated sample of Gly48Met Fyn SH3.[18] Fitting the data together requires a number of assumptions regarding the temperature dependence of rates and chemical shift differences, that in a single temperature, six dispersion study can be completely avoided. Most importantly, the use of ZQ and DQ dispersion profiles allows calculation of the relative signs of $\Delta\varpi_H$ and $\Delta\varpi_N$.[11,19] A central result of this article is that when this information is combined with the sign of $\Delta\varpi_N$, obtained using a generalization of the method of Skrynnikov et al.[20] developed for two-site exchange, *it is possible to reconstruct the ^{1}H$-^{15}$N correlation spectra of the two invisible minor conformations of Gly48Met Fyn SH3, I and U, that are populated at 0.7 and 5%, respectively*. This significantly extends our previous methodology based on ^{15}N SQ data sets where only the signs of ^{15}N chemical shift differences between major and minor conformers could be obtained.[20]

2. Materials and Methods

NMR Spectroscopy. ^{1}H SQ,[11] ^{15}N SQ,[9] ^{1}H$-^{15}$N ZQ,[11] ^{1}H$-^{15}$N DQ,[11] ^{1}H MQ (i.e., ^{1}H$-^{15}$N multiple-quantum with ^{1}H CPMG pulses),[13] and ^{15}N MQ (i.e., ^{1}H$-^{15}$N multiple-quantum with ^{15}N CPMG pulses)[13] relaxation dispersion profiles were recorded on an ^{15}N-labeled, perdeuterated (^{15}N/^{2}H) Gly48Met mutant of the Fyn SH3 domain[21] (0.8 mM protein, 50 mM sodium phosphate, 0.2 mM EDTA, 0.05% NaN_3, 10% D_2O, pH 7) using pulse schemes and experimental parameters described in detail in the cited references. All data sets were measured at field strengths of 11.7, 14.1, and 18.8 T, 25 °C (Figure 1), using Varian *Inova* spectrometers. The intensities of cross-peaks derived from the folded state of Gly48Met Fyn SH3 were quantified using the MUNIN approach.[22,23] Peak intensities obtained from 2D ^{1}H$-^{15}$N spectra were converted into effective relaxation rates, $R_{2,\mathrm{eff}}$, via

$$R_{2,\mathrm{eff}}(\nu_{\mathrm{CPMG}}) = -\frac{1}{T}\ln\frac{I_1(\nu_{\mathrm{CPMG}})}{I_0} \quad (1)$$

where $\nu_{\mathrm{CPMG}} = 1/(4\delta)$, with 2δ the time between application of pulses during the CPMG-type refocusing sequence that is applied during a constant relaxation delay of duration T and $I_1(\nu_{\mathrm{CPMG}})$ and I_0 are the peak intensities in spectra recorded with and without the relaxation delay T, respectively.[24] Uncertainties in $R_{2,\mathrm{eff}}$ were calculated as

$$\Delta R_{2,\mathrm{eff}}(\nu_{\mathrm{CPMG}}) = \frac{1}{T}\frac{\langle\Delta I_1\rangle}{I_1(\nu_{\mathrm{CPMG}})} \quad (2)$$

where $\langle\Delta I_1\rangle$ is the average (over all ν_{CPMG} values) root-mean-squared deviation of peak intensities estimated from repeat measurements.[18] In cases where calculated errors were less than 2% (^{1}H SQ, ^{15}N SQ, ^{1}H MQ, and ^{15}N MQ experiments) or 4% (ZQ and DQ experiments) of $R_{2,\mathrm{eff}}$, a minimum value of 2 or 4%, respectively, was used.

Fitting Relaxation Dispersion Data. Theoretical $R_{2,\mathrm{eff}}^{\mathrm{clc}}$ values were calculated by explicit numerical modeling of magnetization evolution

(17) Tolkatchev, D.; Xu, P.; Ni, F. *J. Am. Chem. Soc.* **2003**, *125*, 12432−12442.
(18) Korzhnev, D. M.; Salvatella, X.; Vendruscolo, M.; Di Nardo, A. A.; Davidson, A. R.; Dobson, C. M.; Kay, L. E. *Nature* **2004**, *430*, 586−590.
(19) Kloiber, K.; Konrat, R. *J. Biomol. NMR* **2000**, *18*, 33−42.
(20) Skrynnikov, N. R.; Dahlquist, F. W.; Kay, L. E. *J. Am. Chem. Soc.* **2002**, *124*, 12352−12360.
(21) Di Nardo, A. A.; Korzhnev, D. M.; Stogios, P. J.; Zarrine-Afsar, A.; Kay, L. E.; Davidson, A. R. *Proc. Natl. Acad. Sci. U.S.A.* **2004**, *101*, 7954−7959.
(22) Orekhov, V. Y.; Ibraghimov, I. V.; Billeter, M. *J. Biomol. NMR* **2001**, *20*, 49−60.
(23) Korzhnev, D. M.; Ibraghimov, I. V.; Billeter, M.; Orekhov, V. Y. *J. Biomol. NMR* **2001**, *21*, 263−268.
(24) Mulder, F. A. A.; Skrynnikov, N. R.; Hon, B.; Dahlquist, F. W.; Kay, L. E. *J. Am. Chem. Soc.* **2001**, *123*, 967−975.

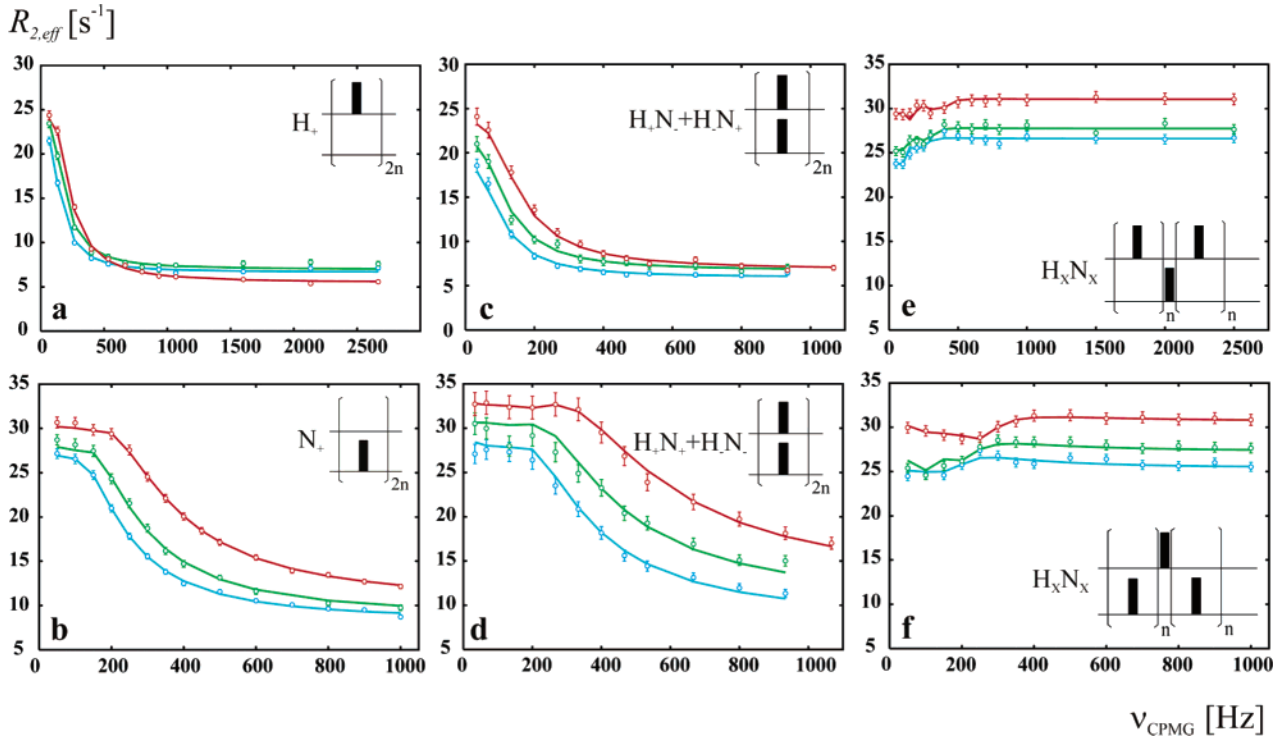

Figure 1. Experimental ^{1}H SQ[10] (TROSY-based[11]) (a), ^{15}N SQ[8,9] (b), ^{1}H−^{15}N ZQ[11] (c), ^{1}H−^{15}N DQ[11] (d), ^{1}H MQ[13] (e), and ^{15}N MQ[13] (f) relaxation dispersion profiles for Asp 9 of the ^{15}N/^{2}H-labeled Gly48Met Fyn SH3 domain (open circles with error bars; 18.8 T red, 14.1T green, 11.7 T blue) and best fits using the "global" three-site exchange model (solid lines). Insets to the plots show simplified schematics of the CPMG-type refocusing elements used in each of the experiments as well as the coherences that evolve during the constant time relaxation period.

during the CPMG-type sequences described above using (i) a model of two-site exchange between folded (F) and unfolded (U) states, F ↔ U, and (ii) a model of three-site exchange that involves an intermediate, I, along the folding trajectory, F ↔ I ↔ U. Details of the $R_{2,eff}$ calculation for the case of two-site exchange are given elsewhere,[7,18] with $R_{2,eff}^{clc}$ calculated for three-site exchange in direct analogy with the two-site case;[18] the theory is summarized in Supporting Information. The parameters of the two-site and three-site exchange models were extracted by least-squares fits of the calculated $R_{2,eff}^{clc}$ values to $R_{2,eff}^{exp}$ rates measured in ^{1}H SQ, ^{15}N SQ, ^{1}H−^{15}N ZQ, ^{1}H−^{15}N DQ, ^{1}H MQ, and ^{15}N MQ experiments by minimization of the following χ^2 target function

$$\chi^2(\zeta) = \sum \frac{(R_{2,eff}^{clc}(\zeta) - R_{2,eff}^{exp})^2}{(\Delta R_{2,eff}^{exp})^2} \qquad (3)$$

where $\zeta = \{x_1, ..., x_{n_{par}}\}$ denotes the set of adjustable model parameters, n_{par} is the number of adjustable model parameters, and the summation in eq 3 is over the number of experimental data points n_{dat}. If the errors in the experimental data are small, normally distributed and uncorrelated with each other, $\chi^2(\zeta)$ at its minimum follows a χ^2 distribution with $\nu = n_{dat} - n_{par}$ degrees of freedom. The quality of data fits was assessed using χ^2 statistics, with model selection (two- versus three-site exchange) based on *F*-test criteria.[25] Uncertainties in the extracted model parameters were estimated using the covariance matrix method,[26] unless indicated otherwise.

The analysis of relaxation dispersion data was performed for 47 of 55 assigned amide resonances of the ^{15}N/^{2}H-labeled Gly48Met mutant of the Fyn SH3 domain. Excluded from the analysis were two pairs of residues whose resonances overlapped in ^{1}H−^{15}N correlation spectra (residues 4, 6 and 16, 32), residues 18 and 25 that show flat dispersions ($R_{2,eff}(\nu_{CPMG})$ measured in at least three of six dispersion experiments is constant with a χ^2 confidence of 1% or higher), and residues 2 and 53. Dispersion profiles for $n_r = 47$ residues measured in $n_c = 6$ relaxation dispersion experiments, each at $n_f = 3$ magnetic fields, were fit together using models of two-site and three-site exchange as described above. Minimization of the "global" χ^2 target function was performed in a space of $n_{dat} = 11\,186$ experimental data points with $n_{par} = n_c \cdot n_r \cdot n_f + 2n_r + 2 = 942$ adjustable parameters, corresponding to $\nu = n_{dat} - n_{par} = 10\,244$ degrees of freedom (two-site exchange model) and with $n_{par} = n_c \cdot n_r \cdot n_f + 4n_r + 4 = 1038$ adjustable parameters and $\nu = n_{dat} - n_{par} = 10\,148$ degrees of freedom (three-site exchange model). The adjustable parameters for the "global" two-state model (F ↔ U) include $n_c \cdot n_r \cdot n_f$ intrinsic (transverse relaxation) R_2 rates (assumed to be the same in F and U states), $2n_r$ chemical shift differences (in ppm) between the exchanging states $\Delta\varpi_{H,FU}$ ($= \varpi_{H,F} - \varpi_{H,U}$) and $\Delta\varpi_{N,FU}$ ($= \varpi_{N,F} - \varpi_{N,U}$), the population of the unfolded state p_U, and the exchange rate constant $k_{ex,FU}$ (sum of folding and unfolding rate constants). The adjustable parameters for the "global" three-state model (F ↔ I ↔ U) are $n_c \cdot n_r \cdot n_f$ intrinsic R_2 rates, $4n_r$ chemical shift differences $\Delta\varpi_{H,FI}$, $\Delta\varpi_{N,FI}$, $\Delta\varpi_{H,FU}$, $\Delta\varpi_{N,FU}$, populations p_I, p_U, and exchange rate constants $k_{ex,FI}$, $k_{ex,IU}$ (sums of forward and reverse rate constants for the reactions F ↔ I and I ↔ U, respectively). Extensive minimizations with different initial conditions were performed to ensure that global minimum χ^2 solutions to fits of dispersion profiles were found, as described below. It is worth noting that we have also fitted the data to a two-site model where the intrinsic transverse relaxation rates differ between sites; however, the reduction in χ^2 was marginal relative to the number of additional parameters that are required, and the model was rejected.

Initial "global" data fits were performed assuming a two-site exchange model using a two-step optimization procedure. First, extensive fits of relaxation dispersion data were performed on a per-residue basis for each of the 47 selected residues. Specifically, experimental ^{1}H SQ, ^{15}N SQ, ^{1}H−^{15}N ZQ, ^{1}H−^{15}N DQ, ^{1}H MQ, and ^{15}N MQ profiles were fit together starting from different initial values

(25) Zar, Z. H. *Biostatistical Analysis*; Prentice Hall Inc.: Englewood Cliffs, NJ, 1984.
(26) Press, W. H.; Flannery, B. P.; Teukolsky, S. A.; Vetterling, W. T. *Numerical Recipes in C*; Cambridge University Press: Cambridge, 1988.

of $\Delta\varpi_{H,FU}$ and $\Delta\varpi_{N,FU}$ (ranging from −1.0 to 1.0 ppm with 0.1 ppm steps for ^{1}H, and from −10 to 10 ppm with 1 ppm steps for ^{15}N) and with reasonable initial estimates of $k_{ex,FU}$ and p_U (e.g., 300 s^{-1} and 3%). Once initial parameters were obtained, relaxation dispersion data for all 47 residues were fit together, using the obtained values of $\Delta\varpi_{H,FU}$, $\Delta\varpi_{N,FU}$, and mean values of $k_{ex,FU}$ and p_U from individual residue fits as starting points.

In the case of data fits to the three-site exchange model (F ↔ I ↔ U), a more complex optimization protocol than the one presented above was necessary. First, to find rough estimates of the exchange rate constants $k_{ex,FI}$, $k_{ex,IU}$ and populations p_I, p_U, an extensive sampling of individual residue χ^2 surfaces as a function of the exchange parameters was performed. Namely, for each residue, a series of χ^2 optimizations were carried out on a grid with fixed values of $k_{ex,FI}$, $k_{ex,IU}$, p_I, p_U ($\log(k_{ex,FI})$, $\log(k_{ex,IU})$ ranging from 2.0 to 4.4 in step sizes of 0.2, p_I, p_U ranging from 0.5 to 10% in steps of 0.5%, $p_I < p_U$) and with $\Delta\varpi_{H,FI}$, $\Delta\varpi_{H,FU}$, $\Delta\varpi_{N,FI}$, $\Delta\varpi_{N,FU}$, and intrinsic R_2 rates minimized. Initial approximations for chemical shift differences in these minimizations were taken from the data analysis using the two-site exchange model F ↔ U (see above). Specifically, χ^2 minimizations were started either from the point where the chemical shifts of the F and I states are identical, $\Delta\varpi_{H,FI} = 0$, $\Delta\varpi_{N,FI} = 0$, $\Delta\varpi_{H,FU} = \Delta\varpi_{H,FU}^{2-site}$, $\Delta\varpi_{N,FU} = \Delta\varpi_{N,FU}^{2-site}$ (referred to in what follows as "01" starts) or from the point where the shifts of states I and U are identical, $\Delta\varpi_{H,FI} = \Delta\varpi_{H,FU} = \Delta\varpi_{H,FU}^{2-site}$, $\Delta\varpi_{N,FI} = \Delta\varpi_{N,FU} = \Delta\varpi_{N,FU}^{2-site}$ ("11" starts). A "global" $\chi^2(k_{ex,FI}, k_{ex,IU}, p_I, p_U)$ surface (sampled at 27 360 discrete points) was subsequently generated for all 47 residues of Gly48Met Fyn SH3 by adding the per-residue χ^2 values (two separate "global" χ^2 surfaces were obtained, corresponding to "01" and "11" starts). Note that, at this point, values of chemical shift differences and intrinsic rates have been minimized using the three-site model for each of the points on the grid. The 20 combinations of $k_{ex,FI}$, $k_{ex,IU}$, p_I, p_U (for each "01" and "11" start) that resulted in the lowest "global" χ^2 values, along with the corresponding shift values, $\Delta\varpi_{H,FI}$, $\Delta\varpi_{H,FU}$, $\Delta\varpi_{N,FI}$, $\Delta\varpi_{N,FU}$, and intrinsic R_2 rates obtained from the per-residue three-site fits, were used as starting points for subsequent optimizations of the "global" χ^2 target function that involved all 47 residues (six coherences, three fields) and for which *all* model parameters were adjusted. Most "global" minimizations performed in this way converge to the same solution locus (i.e., result in about the same χ^2 values and in very similar three-site exchange parameters). The parameters generated from the "global" three-site solution with the lowest χ^2 were used in all subsequent analyses.

Simulations To Establish the Robustness of the Three-Site Solution. To ensure that the exchange parameters that were obtained from the fits described above were not the result of one or two pathological residues, we have carried out 25 jackknife simulations.[26] In each of these computations, the experimental relaxation dispersion data for a random subset of residues (10 out of 47) were excluded from data analysis, and the protocol described in the previous section was repeated for the reduced set of residues ("01" starts only); for each simulation the solution with the lowest "global" χ^2 value was retained for further analysis.

Similarly, the influence of random errors in experimental $R_{2,eff}$ values on the "global" three-site solution was assessed by 20 Monte Carlo simulations.[26] For each of these 20 runs, exact synthetic dispersion data were generated for 47 residues based on the parameters obtained in the "global" fit of the experimental data (see above), and to these data was added random noise with a standard deviation of 2% (^{1}H SQ, ^{15}N SQ, ^{1}H MQ, and ^{15}N MQ data) or 4% (^{1}H−^{15}N ZQ and ^{1}H−^{15}N DQ data). Again, global optimization was performed according to the above protocol ("01" starts only), with the lowest "global" χ^2 solution retained from each run.

3. Results and Discussion

Six Types of Relaxation Dispersion Data for Backbone Amide Groups of Proteins. Figure 1 shows ^{1}H SQ (a), ^{15}N SQ (b), ^{1}H−^{15}N ZQ (c), ^{1}H−^{15}N DQ (d), ^{1}H MQ (e), and ^{15}N MQ (f) dispersion profiles for Asp9 of ^{15}N/^{2}H, Gly48Met Fyn SH3. The coherences that evolve during the CPMG period, along with the type of CPMG-refocusing schemes that have been used in each of the relaxation dispersion experiments, are indicated as insets in each of the panels. In the conventional ^{1}H and ^{15}N SQ schemes,[9,10,27] or their TROSY counterparts,[11,27] a CPMG pulse train is applied to either ^{1}H or ^{15}N spins after creating the desired single-quantum coherence (for simplicity labeled as H_+ and N_+ in Figure 1a,b). In the ^{1}H−^{15}N ZQ and ^{1}H−^{15}N DQ schemes,[11] a CPMG-type refocusing sequence with simultaneous ^{1}H and ^{15}N 180° pulses is applied to either zero-quantum $H_+N_- + H_-N_+$ or double-quantum $H_+N_+ + H_-N_-$ coherences (Figure 1c,d). In ^{1}H MQ and ^{15}N MQ experiments,[13] CPMG trains of ^{1}H 180° (^{1}H MQ) or ^{15}N 180° (^{15}N MQ) pulses are applied to multiple-quantum coherence, H_xN_x, that consists of a 1:1 combination of double- and zero-quantum coherences $(H_+N_+ + H_+N_- + H_-N_+ + H_-N_-)/4$, with a single ^{15}N 180° pulse (^{1}H MQ scheme) or ^{1}H 180° pulse (^{15}N MQ scheme) applied at the midpoint of the constant relaxation time CPMG interval to refocus evolution due to ^{15}N or ^{1}H chemical shift, respectively (Figure 1e,f).

The CPMG frequency (ν_{CPMG}) dependence of the $R_{2,eff}$ rates obtained in ^{1}H SQ, ^{15}N SQ, ^{1}H−^{15}N ZQ, and ^{1}H−^{15}N DQ dispersion experiments can be expressed by a set of analogous equations[28,29] that depend on exchange parameters in the same way (see Supporting Information). Thus, in the case of two-site exchange between states F and U, the dispersion profiles $R_{2,eff}(\nu_{CPMG})$ depend on the forward and reverse rate constants k_{FU} and k_{UF} (or, equivalently, on the population of state U, p_U, and the exchange rate constant $k_{ex} = k_{FU} + k_{UF}$) and on the absolute value of the frequency difference between the exchanging states $|\Delta\omega|$, where $\Delta\omega$ is $\Delta\omega_{H,FU}$, $\Delta\omega_{N,FU}$, $\Delta\omega_{H,FU} - \Delta\omega_{N,FU}$, and $\Delta\omega_{H,FU} + \Delta\omega_{N,FU}$ for dispersion curves of the ^{1}H SQ, ^{15}N SQ, ^{1}H−^{15}N ZQ, and ^{1}H−^{15}N DQ variety, respectively. In what follows, we will distinguish between chemical shift differences in rad/s ($\Delta\omega$) from those in ppm ($\Delta\varpi$), with the relation between the two defined according to $\Delta\omega_{H,FU} = \omega_H\Delta\varpi_{H,FU}$, $\Delta\omega_{N,FU} = \omega_N\Delta\varpi_{N,FU}$, with ω_H and ω_N the Larmor frequencies of ^{1}H and ^{15}N nuclei, respectively. In contrast, the description of MQ dispersion profiles is slightly more complex (see Supporting Information), since evolution of both ^{1}H and ^{15}N spins occurs during the CPMG element and a refocusing pulse train is applied to either ^{1}H or ^{15}N (but not both). Not surprisingly, MQ dispersion profiles are sensitive to changes in the chemical environments of *both* ^{1}H and ^{15}N spins.[13,30] In the special case where $\Delta\omega_{H,FU} = 0$, $\Delta\omega_{N,FU} \neq 0$ ($\Delta\omega_{H,FU} \neq 0$, $\Delta\omega_{N,FU} = 0$) ^{15}N (^{1}H) MQ dispersion profiles are identical to those obtained in ^{15}N (^{1}H) SQ experiments (see figures in Supporting Information); however, when $|\Delta\omega_{H,FU}| \approx |\Delta\omega_{N,FU}|$ ^{15}N and ^{1}H MQ profiles behave quite differently than their SQ counterparts and can even increase as a function of ν_{CPMG}[13] (e.g., Figure 1e,f).

As mentioned in the Introduction, the combined analysis of the six relaxation dispersion profiles that have been obtained for each residue in the case of the ^{15}N/^{2}H Gly48Met domain

(27) Loria, J. P.; Rance, M.; Palmer, A. G. *J. Biomol. NMR* **1999**, *15*, 151−155.
(28) Carver, J. P.; Richards, R. E. *J. Magn. Reson.* **1972**, *6*, 89−105.
(29) Jen, J. *J. Magn. Reson.* **1978**, *30*, 111−128.
(30) Korzhnev, D. M.; Kloiber, K.; Kanelis, V.; Tugarinov, V.; Kay, L. E. *J. Am. Chem. Soc.* **2004**, *126*, 3964−3973.

Table 1. Conformational Exchange Parameters Obtained from an Analysis of Six Dispersion Profiles/Residue for 47 Residues of $^{15}N/^{2}H$ Gly48Met Fyn SH3 Using "Global" Two-Site and Three-Site Exchange Models[a]

model	p (%)	k_{ex} (s^{-1})	χ^2/#DF[b]	$P(\chi^2)$
two-site	5.21 ± 0.04 (U)	378 ± 3 (FU)	13542/10244	0
three-site best fit	0.73 ± 0.04 (I) 5.13 ± 0.05 (U)	4673 ± 382 (FI) 6756 ± 231 (IU)	9651/10148	0.9998
three-site jackknife	0.69 ± 0.06 (I) 5.18 ± 0.06 (U)	5324 ± 665 (FI) 6795 ± 774 (IU)		

[a] Shown are the best-fit values for the populations of the exchanging states p_U (two-site model) and p_I, p_U (three-site model), exchange rate constants $k_{ex,FU}$ (two-site) and $k_{ex,FI}$, $k_{ex,FU}$ (three-site), "global" χ^2 target functions and the number of degrees of freedom, #DF, and confidence level for the χ^2 values at the given number of degrees of freedom, $P(\chi^2)$. Also included are the mean parameters obtained from the jackknife simulation ± standard deviations (see Materials and Methods for details). [b] An F-test analysis shows that the probability that the observed reduction in χ^2 obtained when the data is fit to the more complex (three-site) model being due to chance is zero.

provides a more quantitative picture of the exchange dynamics than that obtained from our previous ^{15}N dispersion study of a fully protonated version of the protein.[18] First, the use of deuteration facilitates the measurement of dispersion profiles involving the application of ^{1}H refocusing pulses during the CPMG pulse train; the effects of $^{1}H-^{1}H$ cross-relaxation and scalar coupling that manifest in protonated samples and that can vary as a function of the number of ^{1}H pulses can be significantly minimized or eliminated in highly deuterated samples.[10] Second, it is possible to employ values of ν_{CPMG} in ^{1}H SQ and MQ schemes (50 Hz to 2.5−3 kHz) that are severalfold larger than generally used in ^{15}N SQ experiments (50 Hz to 1 kHz). This increases the sensitivity of the ^{1}H experiments to exchange processes over a wider range of time scales. On a related note, amide proton chemical shifts can be more sensitive to the changes in protein conformation than their ^{15}N counterparts, since, for example, the dispersion of $^{1}H^{N}$ chemical shifts for amino acids of the same type (expressed in Hz) is, on average, 1.6 times higher than for ^{15}N nuclei.[31] Third, all six types of dispersion profiles depend on the same set of parameters that are required to fit ^{15}N and ^{1}H SQ data. Computations have clearly shown that the additional data leads to more robust estimates of the exchange parameters (manuscript in progress), with data sets composed of ^{1}H and ^{15}N dispersion profiles exclusively already representing a significant improvement relative to the case where only ^{15}N data is considered. Finally, the ZQ/DQ dispersion profiles are uniquely sensitive to the relative signs of $\Delta\omega_H$ and $\Delta\omega_N$,[19] and this sign information is an important component in the reconstruction of $^{1}H-^{15}N$ correlation spectra of the invisible, excited states (see below).

Optimal Parameters of the Two-Site and Three-Site Exchange Models. As described in Materials and Methods, a global fit involving six relaxation dispersion profiles measured at three static magnetic fields for 47 well-resolved residues of $^{15}N/^{2}H$ Gly48Met Fyn SH3 was performed using models of two-site, F ↔ U, and three-site, F ↔ I ↔ U, exchange. Conformational exchange parameters and χ^2 values obtained in the "global" data fits are summarized in Table 1. According to χ^2 statistical criteria, the data are not well fit to a two-site model (the "global" two-site χ^2 value exceeds the number of degrees of freedom, χ^2 confidence $P(\chi^2) \approx 0$), while the three-site model is able to account for the data ($P(\chi^2) \approx 1$). Because the actual value of the χ^2 target function (eq 3) strongly depends on the estimated uncertainties in the experimental data, a comparison of the data fits has been made using the *F*-test criterion,[26] showing that the three-site model provides a statistically significant improvement in fit relative to that obtained via the two-site model (χ^2 drops by 4000 with only 96 additional adjustable parameters added, *F*-test confidence ≈ 1, see Table 1).

Previous experiments have clearly shown that deuteration of carbon positions reduces the stability of folded proteins, due to a decrease in the polarizability of $^{13}C-^{2}H$ versus $^{13}C-^{1}H$ bonds that leads to a weakening of van der Waals interactions.[32−34] Such an effect is clearly observed in the data presented here. For deuterated Gly48Met Fyn SH3, a decrease in stability of both the folded (F) and intermediate (I) states (relative to U) is noted in comparison with the protonated version of the molecule. For example, in the protonated protein the populations of states I and U are 1.2 and 1.9%, respectively[18] (25 °C), while I and U are populated to 0.7 and 5.1% in the deuterated sample (Table 1). The corresponding exchange rate constants between F and I and between I and U become faster in the deuterated protein ($k_{ex,FI} = 4673\ s^{-1}$, $k_{ex,IU} = 6756\ s^{-1}$ versus $k_{ex,FI} = 1546\ s^{-1}$, $k_{ex,IU} = 5026\ s^{-1}$ in protonated form). The overall folding reaction, as viewed from the perspective of a two-state F ↔ U model, becomes slower as a result of deuteration, with $k_{ex,FU}^{2-site}$ values of 378 and 532 s^{-1} measured for the deuterated and protonated molecules, respectively, at 25 °C.

Reconstruction of Spectra of the Low Populated I and U States. The first step in any NMR study involves recording spectra and assigning the resulting correlations to specific sites in the molecule.[35] These assignments then serve as the starting point for detailed structural, dynamic, and thermodynamic investigations of the system in hand. In the case of studies of "invisible" excited protein states, it is evident that the situation is more complex. Clearly, an approach for the *complete* reconstruction of $^{1}H-^{15}N$ (or $^{1}H-^{13}C$) correlation maps of these low populated states would be of great interest. To put our approach into context, consider first a two-site exchange process, F ↔ U, and suppose that all six dispersion profiles discussed above have been recorded. The ^{1}H, ^{15}N SQ, and the $^{1}H,^{15}N$ MQ data sets are sensitive to the absolute values of chemical shift differences between the exchanging states,[6,28] $|\Delta\varpi_{H,FU}|$ and $|\Delta\varpi_{N,FU}|$. Thus, if the ^{15}N SQ data were to be fit independently, a pair of solutions with equivalent χ^2 values corresponding to shift differences of $\pm\Delta\varpi_{N,FU}$ would be obtained. Likewise, simultaneous fits of ^{1}H, ^{15}N SQ and ^{1}H, ^{15}N MQ dispersion profiles yield four chemical shift combinations that are indistinguishable in terms of goodness of fit: 1: ($\Delta\varpi_{H,FU}$, $\Delta\varpi_{N,FU}$), 2: ($\Delta\varpi_{H,FU}$, $-\Delta\varpi_{N,FU}$), 3: ($-\Delta\varpi_{H,FU}$, $\Delta\varpi_{N,FU}$), and 4: ($-\Delta\varpi_{H,FU}$, $-\Delta\varpi_{N,FU}$). The 4-fold ambiguity can be reduced by a factor of 2 by recording $^{1}H-^{15}N$ ZQ, DQ dispersion

(31) Doreleijers, J. F.; Mading, S.; Maziuk, D.; Sojourner, K.; Yin, L.; Zhu, J.; Markley, J. L.; Ulrich, E. L. *J. Biomol. NMR* **2003**, *26*, 139−146.
(32) Turowski, M.; Yamakawa, N.; Meller, J.; Kimata, K.; Ikegami, T.; Hosoya, K.; Tanaka, N.; Thornton, E. R. *J. Am. Chem. Soc.* **2003**, *125*, 13836−13849.
(33) Hattori, A.; Crespi, H. L.; Katz, J. J. *Biochemistry* **1965**, *12*, 13−25.
(34) Rokop, S.; Gajda, L.; Parmerter, S.; Crespi, H. L.; Katz, J. J. *Biochim. Biophys. Acta* **1969**, *191*, 707−715.
(35) Wüthrich, K. *NMR of Proteins and Nucleic Acids*; Wiley & Sons: New York, 1986.

curves[11,12] that depend on absolute values of frequency differences $|\Delta\omega_{FU}^{ZQ}|$ and $|\Delta\omega_{FU}^{DQ}|$ given by $|\Delta\omega_{H,FU} - \Delta\omega_{N,FU}|$ and $|\Delta\omega_{H,FU} + \Delta\omega_{N,FU}|$, respectively. In this way, the ZQ and DQ profiles establish the relative signs of $\Delta\varpi_{H,FU}$, $\Delta\varpi_{N,FU}$[19] so that, if solution 1 satisfies the ZQ and DQ data then so will solution 4, but not 2 and 3. Thus, the combined analysis of six types of dispersion data results in *two* indistinguishable combinations of chemical shift differences between the exchanging states where if ($\Delta\varpi_{H,FU}$, $\Delta\varpi_{N,FU}$) is a solution, then so too is ($-\Delta\varpi_{H,FU}$, $-\Delta\varpi_{N,FU}$).

The two solutions mentioned above can be discriminated by measuring the signs of the ^{15}N chemical shift differences between corresponding resonances in states F and U, $\Delta\varpi_{N,FU}$, using the approach of Skrynnikov et al.[20] (recall that the resonances in state U are invisible!). In this method, the signs of $\Delta\varpi_{N,FU}$ are obtained from a comparison of peak positions in ^{1}H$-^{15}$N HSQC spectra recorded at different magnetic fields, noting that the correlation from the F state will move closer to the U state (in ppm) in the lower field map. Thus, the difference between ^{15}N chemical shifts of the resonances of state F obtained in HSQC spectra recorded at 18.8 and 11.7 T fields, $\delta_{EXP} = \varpi_{18.8} - \varpi_{11.7}$, will have the same sign as $\Delta\varpi_{N,FU} = \varpi_{N,F} - \varpi_{N,U}$.

Consider now the case of three-site exchange, F $\leftrightarrow$ I $\leftrightarrow$ U. In an analogous manner to what is observed in the two-site case, fits involving ^{15}N SQ data exclusively give two solutions with the same χ^2 value so that if ($\Delta\varpi_{N,FI}$, $\Delta\varpi_{N,FU}$) is one such solution then ($-\Delta\varpi_{N,FI}$, $-\Delta\varpi_{N,FU}$) will be the second (note that if ($\Delta\varpi_{N,FI}$, $\Delta\varpi_{N,FU}$) is a solution then ($\Delta\varpi_{N,FI}$, $-\Delta\varpi_{N,FU}$) and ($-\Delta\varpi_{N,FI}$, $\Delta\varpi_{N,FU}$) will not be). Simultaneous fits of ^{1}H,^{15}N SQ and ^{1}H,^{15}N MQ data sets yield four equivalent solutions, and if ($\Delta\varpi_{H,FI}$, $\Delta\varpi_{H,FU}$, $\Delta\varpi_{N,FI}$, $\Delta\varpi_{N,FU}$) is one then so too will be ($\Delta\varpi_{H,FI}$, $\Delta\varpi_{H,FU}$, $-\Delta\varpi_{N,FI}$, $-\Delta\varpi_{N,FU}$), ($-\Delta\varpi_{H,FI}$, $-\Delta\varpi_{H,FU}$, $\Delta\varpi_{N,FI}$, $\Delta\varpi_{N,FU}$), and ($-\Delta\varpi_{H,FI}$, $-\Delta\varpi_{H,FU}$, $-\Delta\varpi_{N,FI}$, $-\Delta\varpi_{N,FU}$). Two of these solutions can be eliminated based on ^{1}H$-^{15}$N ZQ and DQ profiles. Again, if ($\Delta\varpi_{H,FI}$, $\Delta\varpi_{H,FU}$, $\Delta\varpi_{N,FI}$, $\Delta\varpi_{N,FU}$) is a solution based on a combined analysis of all six dispersion profiles then ($-\Delta\varpi_{H,FI}$, $-\Delta\varpi_{H,FU}$, $-\Delta\varpi_{N,FI}$, $-\Delta\varpi_{N,FU}$) will also satisfy the dispersions with an equivalent χ^2 value. These two solutions, can, however, be distinguished by calculating the signs of $\Delta\varpi_{N,FI}$ and $\Delta\varpi_{N,FU}$ on the basis of an extension of the approach of Skrynnikov et al.[20] as explained below.

The evolution of ^{15}N transverse magnetization during the t_1 period of an HSQC experiment (neglecting ^{1}H$-^{15}$N scalar coupling) in a system undergoing exchange between a populated state F and a pair of minor states I and U (F $\leftrightarrow$ I $\leftrightarrow$ U) is given by

$$\frac{d}{dt}\begin{bmatrix} M_{F+} \\ M_{I+} \\ M_{U+} \end{bmatrix} = \begin{bmatrix} -R_{2F} - k_{FI} & k_{IF} & 0 \\ k_{FI} & -R_{2I} - k_{IF} - k_{IU} - i\Delta\omega_{N,FI} & k_{UI} \\ 0 & k_{IU} & -R_{2U} - k_{UI} - i\Delta\omega_{N,FU} \end{bmatrix} \begin{bmatrix} M_{F+} \\ M_{I+} \\ M_{U+} \end{bmatrix} \quad (4)$$

where M_j is the magnetization associated with state j, $M_+ = M_x + iM_y$, the frequency difference between corresponding resonances in states k and l ($\omega_k - \omega_l$) is $\Delta\omega_{N,kl} = \omega_N\Delta\varpi_{N,kl}$, $\omega_N = -\gamma_N B_0$ is the field-dependent Larmor frequency of the ^{15}N spin, and the resonance frequency of state F is assumed to be equal to 0. The F_1 resonance frequency of a correlation derived from the major state (F) in the spectrum is given by $\varpi = \mathrm{Im}(\lambda_1)/\omega_N$, where λ_1, λ_2, and λ_3 are the eigenvalues of the evolution matrix of eq 4 and $|\mathrm{Im}(\lambda_1)| < |\mathrm{Im}(\lambda_2)|, |\mathrm{Im}(\lambda_3)|$. Thus, the F_1 peak position of the major state is shifted with respect to the resonance frequency of state F (i.e., in the absence of exchange) in a manner dependent on the frequencies of states I and U and on the parameters that describe the exchange process. It is this dependence that provides the information necessary to distinguish between the two remaining solutions.

For each of the two possible solutions ($\Delta\varpi_{H,FI}$, $\Delta\varpi_{H,FU}$, $\Delta\varpi_{N,FI}$, $\Delta\varpi_{N,FU}$) and ($-\Delta\varpi_{H,FI}$, $-\Delta\varpi_{H,FU}$, $-\Delta\varpi_{N,FI}$, $-\Delta\varpi_{N,FU}$) discussed above, the F_1 peak position of the major state is calculated from λ_1 (eq 4) using the exchange parameters obtained from the "global" three-site fit of the relaxation dispersion data. This process is repeated for a pair of spectrometer field strengths (in our case 11.7 and 18.8 T), and the expected field-dependent shift in peak positions (ppm), δ_{CLC}, is obtained. The value of δ_{CLC} is compared with that observed experimentally, $\delta_{EXP} = \varpi_{18.8} - \varpi_{11.7}$ (ppm); only one of the chemical shift solutions will produce a δ_{CLC} value that agrees with experiment. A comparison of δ_{CLC} and δ_{EXP} is made for each of the 47 selected residues of the ^{15}N/^{2}H Gly48Met Fyn SH3 domain, providing the signed shift differences for each backbone ^{1}H$-^{15}$N spin pair.

To minimize any systematic shifts in the HSQC data sets recorded at the two fields that might originate from subtle differences in experimental conditions, a set of amide resonances from the His-tag region of the SH3 domain construct that produces flat dispersion profiles was used as a reference, with the difference between shifts of these residues in the two HSQCs minimized. Values of δ_{EXP}, ranging from -0.02 to 0.02 ppm have been observed, with an excellent correlation between δ_{EXP} and δ_{CLC} (inset to Figure 2a). Thus, the signs of $\Delta\varpi_{H,FI}$, $\Delta\varpi_{H,FU}$, $\Delta\varpi_{N,FI}$, $\Delta\varpi_{N,FU}$ can be unambiguously obtained, even for residues with small values of $\Delta\varpi_{N,FU}$. The signs of $\Delta\varpi$ were confirmed by the ^{1}H chemical shifts of state U obtained from $\Delta\varpi_{H,FU}$ that, of course, must correspond to the values expected for an unfolded protein. Unreasonable ^{1}H chemical shifts in state U have been observed for only two of six residues with $|\Delta\varpi_{N,FU}| < 0.5$ ppm, shown in red in Figure 2. For these residues (Lys 22 and Met 48 that have $|\Delta\varpi_{N,FU}| < 0.32$ ppm), the signs of all $\Delta\varpi$ have been corrected (i.e., inverted). In principle, the signs of $\Delta\varpi_{H,FI}$ and $\Delta\varpi_{H,FU}$ could also be calculated from peak shifts along the ^{1}H dimension of HSQC spectra; however, for yet unknown reasons a very poor correlation between ^{1}H δ_{EXP} and δ_{CLC} has been observed.

Figure 2a shows the experimental ^{1}H$-^{15}$N correlation map of the F state of the ^{15}N/^{2}H Gly48Met Fyn SH3 domain, with the *reconstructed* ^{1}H$-^{15}$N correlation spectra for states I and U shown in parts b and c of Figure 2, respectively (for the 47 selected amide resonances with reliable dispersion data). Also shown as insets (Figure 2b,c) are the correlations of the experimental ^{15}N chemical shifts of states I and U, $\varpi_{I,EXP}$ and $\varpi_{U,EXP}$, with the ^{15}N chemical shifts of the unfolded state of Gly48Met Fyn SH3, $\varpi_{U,CLC}$, calculated using the CSI module in the NMRView program.[36,37] It is clear that the spectrum of

(36) Johnson, B. A.; Blevins, R. A. *J. Biomol. NMR* **1994**, *4*, 603−614.

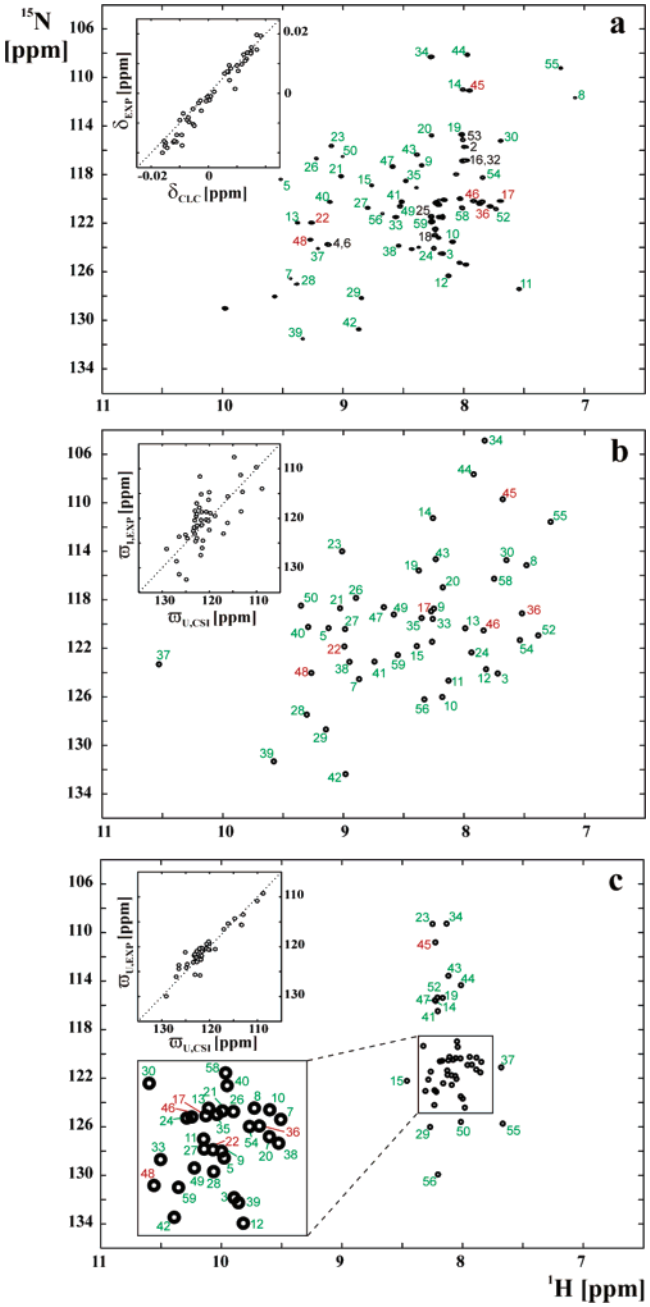

Figure 2. Experimental ^{1}H−^{15}N HSQC spectrum of the F state (a), and reconstructed spectra of states I (b) and U (c) of ^{15}N/^{2}H Gly48Met Fyn SH3, 25 °C. For I and U states, 47 correlations (out of a total of 55 assigned amide resonances) were used in the analysis of relaxation dispersion data (green and red residue numbers, with red marking those residues with $|\Delta\omega_{N,FU}| < 0.5$; black numbers in plot *a* identify residues that were excluded from the analysis; see text for details). Spectra of states I and U were reconstructed as described in the text. Inset to plot *a* shows the correlation between peak shifts along F_1 in HSQC spectra measured at 11.7 and 18.8 T, δ_{EXP}, with peak shifts calculated using eq 4 based on exchange parameters obtained in the "global" three-site fit of relaxation dispersion data, δ_{CLC}. Insets to plots *b* and *c* show correlations of ^{15}N chemical shifts for states I and U, $\varpi_{I,EXP}$ and $\varpi_{U,EXP}$, with ^{15}N chemical shifts of the unfolded state of Gly48Met Fyn SH3 predicted using the CSI module of NMRView,[36,37] $\varpi_{U,CLC}$.

the U state resembles that of an unfolded protein, and a good correlation between $\varpi_{U,EXP}$ and $\varpi_{U,CLC}$ is observed, whereas the spectrum of the I state is well-dispersed. The ^{1}H and ^{15}N chemical shifts of the F state along with the signed chemical shift differences between states F and I, and F and U, $\Delta\varpi_{H,FI}$,

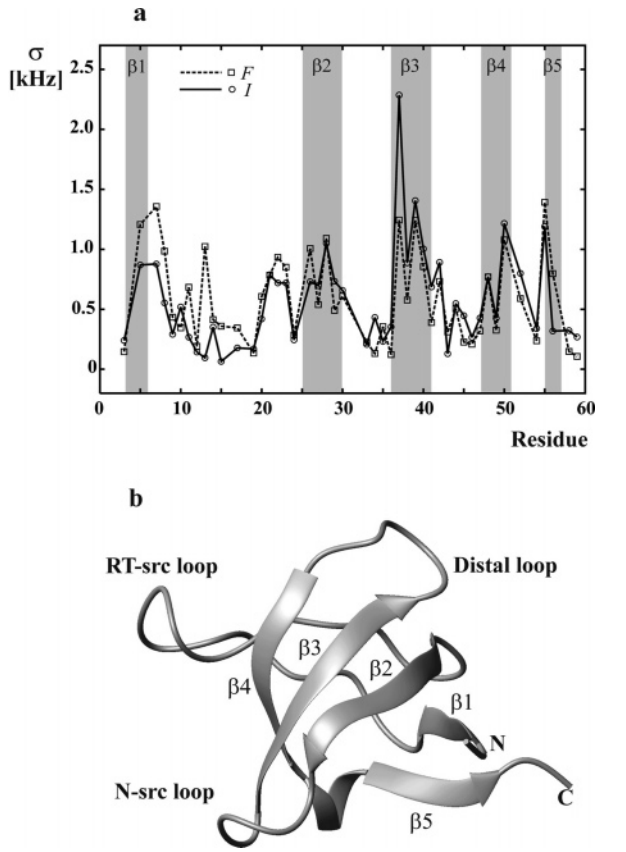

Figure 3. (a) Deviations from unfolded backbone chemical shifts for the intermediate I, $2\pi\sigma_I = (\Delta\omega_{H,IU}^2 + \Delta\omega_{N,IU}^2)^{1/2}$ (solid lines, open circles) and folded F, $2\pi\sigma_F = (\Delta\omega_{H,FU}^2 + \Delta\omega_{N,FU}^2)^{1/2}$ (dashed lines, open boxes), states of ^{15}N/^{2}H Gly48Met Fyn SH3, respectively, expressed in absolute frequency units at a magnetic field of 18.8 T. (b) Ribbon diagram of the folded structure of the WT Fyn SH3 domain, PDB accession number 1SHF.[38]

$\Delta\varpi_{N,FI}$, $\Delta\varpi_{H,FU}$, and $\Delta\varpi_{N,FU}$ obtained from the "global" fit of the six relaxation dispersion profiles per residue using the three-site exchange model are summarized in Table 2. It bears repeating at this stage that both I (0.7%) and U (5.1%) states are invisible in spectra; nevertheless, the approach described above has allowed the near-complete reconstruction of their ^{1}H−^{15}N correlation maps.

Structural Information about the I State from Chemical Shifts. The chemical shifts and chemical shift differences shown in Table 2 provide structural information about the low populated I and U states of the ^{15}N/^{2}H Gly48Met Fyn SH3 domain. For example, the ^{15}N chemical shifts of state U, $\varpi_{U,EXP}$, derived from the chemical shifts of state F and the chemical shift differences $\Delta\varpi_{N,FU}$, are very similar to those of a random coil (see inset to Figure 2c). Insight into the structure of the I state can be obtained from a comparison of the chemical shifts of state I with the shifts of states F and U, in a manner similar to that described previously in the context of our ^{15}N dispersion study of a protonated Gly48Met Fyn SH3 domain.[18] However, the new information obtained in this work, namely the amide proton chemical shift differences between the exchanging states, $\Delta\varpi_{H,FI}$, $\Delta\varpi_{H,FU}$, is potentially more sensitive to changes in

(37) Schwarzinger, S.; Kroon, G. J.; Foss, T. R.; Chung, J.; Wright, P. E.; Dyson, H. J. *J. Am. Chem. Soc.* **2001**, *123*, 2970−2978.
(38) Noble, M. E.; Musacchio, A.; Saraste, M.; Courtneidge, S. A.; Wierenga, R. K. *EMBO J.* **1993**, *12*, 2617−2624.

Table 2. ^{15}N and ^{1}H Chemical Shifts, ϖ_N and ϖ_H, of the Folded State (F) and ^{15}N and ^{1}H Chemical Shift Differences between Folded and Intermediate ($\Delta\varpi_{N,FI}$ and $\Delta\varpi_{H,FI}$) and between Folded and Unfolded States ($\Delta\varpi_{N,FU}$ and $\Delta\varpi_{H,FU}$) for 47 Residues of ^{15}N/^{2}H-Labeled G48M Fyn SH3 Obtained in the Analysis of ^{1}H SQ, ^{15}N SQ, ^{1}H−^{15}N ZQ, ^{1}H−^{15}N DQ, ^{1}H MQ, and ^{15}N MQ Relaxation Dispersion Data at 25 °C Using a Three-Site Exchange Model ($F \leftrightarrow I \leftrightarrow U$)

residue	ϖ_N	ϖ_H	$\Delta\varpi_{N,FI}$	$\Delta\varpi_{N,FU}$	$\Delta\varpi_{H,FI}$	$\Delta\varpi_{H,FU}$	residue	ϖ_N	ϖ_H	$\Delta\varpi_{N,FI}$	$\Delta\varpi_{N,FU}$	$\Delta\varpi_{H,FI}$	$\Delta\varpi_{H,FU}$
3	124.52	8.166	0.44	1.01	0.445	0.151	34	108.30	8.264	3.43	−0.97	0.435	0.131
5	118.40	9.514	−1.94	−3.66	0.391	1.463	35	118.53	8.475	−0.98	−1.95	0.124	0.397
7	126.57	9.432	2.03	5.91	0.563	1.587	36	120.62	7.772	1.50	−0.27	0.253	−0.150
8	111.68	7.068	−3.47	−8.57	−0.414	−0.873	37	124.10	9.205	0.78	2.99	−1.324	1.525
9	117.24	8.342	−1.48	−4.57	0.093	0.281	38	123.86	8.533	0.75	2.35	−0.416	0.681
10	123.20	8.200	−2.81	2.90	0.021	0.315	39	131.53	9.331	0.22	7.85	−0.246	1.332
11	127.43	7.533	2.77	6.06	−0.595	−0.593	40	120.26	9.106	0.02	0.83	−0.186	1.066
12	126.34	8.120	2.63	1.92	0.303	0.138	41	120.24	8.508	−2.85	3.76	−0.233	0.303
13	121.98	9.375	1.63	1.73	1.385	1.267	42	130.75	8.866	−1.62	6.54	−0.115	0.632
14	110.99	8.002	−0.26	−4.58	−0.254	−0.226	43	116.36	8.382	1.71	2.80	0.148	0.265
15	118.89	8.758	−2.93	−3.33	0.367	0.297	44	108.14	7.963	0.49	−6.20	0.044	−0.050
17	120.18	7.689	1.23	−0.34	−0.584	−0.429	45	111.09	7.944	1.39	0.28	0.266	−0.281
19	114.69	8.010	−0.89	−0.68	−0.365	−0.155	46	120.18	7.912	−0.34	−0.39	0.074	−0.258
20	114.78	8.262	−2.20	−6.51	0.085	0.375	47	117.35	8.584	−1.26	1.72	−0.080	0.361
21	118.13	9.011	−0.56	−2.21	−0.016	0.954	48	123.37	9.269	−0.66	0.32	0.003	0.962
22	121.96	9.258	0.12	0.21	0.267	1.166	49	120.62	8.524	1.41	−1.80	−0.057	0.363
23	115.65	9.094	1.64	6.36	0.084	0.845	50	116.51	8.999	−1.97	−9.09	−0.353	0.985
24	124.08	8.242	1.74	3.47	0.304	0.054	52	120.85	7.725	−0.08	5.49	0.340	−0.483
26	116.68	9.218	−1.16	−3.69	0.324	1.201	54	118.26	7.835	−3.07	−2.65	0.299	−0.124
27	120.74	8.790	0.32	−0.99	−0.196	0.665	55	109.23	7.187	−2.32	−16.51	−0.095	−0.481
28	127.02	9.377	−0.45	4.46	0.073	1.287	56	121.22	8.667	−4.99	−8.72	0.338	0.464
29	128.17	8.842	−0.51	2.16	−0.303	0.573	58	120.75	8.004	4.49	1.78	0.253	−0.042
30	115.23	7.686	0.49	−4.12	0.038	−0.639	59	121.89	8.263	−0.66	−1.23	−0.286	0.045
33	121.50	8.558	1.93	−0.61	0.300	0.275							

protein structure than the ^{15}N shift differences, $\Delta\varpi_{N,FI}$, $\Delta\varpi_{N,FU}$[31] that were obtained before (see discussion above).

Figure 3a shows deviations of the chemical shifts of the intermediate I ($2\pi\sigma_I = (\Delta\omega_{H,IU}^2 + \Delta\omega_{N,IU}^2)^{1/2}$) and folded F ($2\pi\sigma_F = (\Delta\omega_{H,FU}^2 + \Delta\omega_{N,FU}^2)^{1/2}$) states relative to the U state, expressed in absolute frequency units (Hz) at a magnetic field of 18.8 T. A reasonably good correlation between σ_I and σ_F values is observed in β-strands 2, 3, and 4 (Figure 3b) and in the distal and N-src loops (except for several residues in β3 where $\sigma_I > \sigma_F$), suggesting the formation of a nativelike structure in this region of the I state (i.e., the small chemical shift differences between states I and F are localized[18]). In contrast, values of $\sigma_I < \sigma_F$ obtained for residues in β1, β5, and the RT-src loop imply that the structure in these regions is likely more disordered in the I state. This picture, based on the analysis of both ^{1}H and ^{15}N chemical shift differences, is in qualitative agreement with the results of our previous ^{15}N study of a fully protonated domain.[18]

Figure 4 compares the ^{15}N chemical shift differences (in ppm), $\Delta\varpi_{N,FU}$, $\Delta\varpi_{N,FI}$, obtained from analyses of the relaxation data measured on the deuterated (six dispersion profiles per residue, 25 °C) and fully protonated (^{15}N SQ data, five temperatures) Gly48Met Fyn SH3 domains. The agreement between $\Delta\varpi_{N,FU}$ values (Figure 4a) is excellent, with a much more modest correlation observed for $\Delta\varpi_{N,FI}$ (Figure 4b). Notably, values of $\Delta\varpi_{N,FI}$ are considerably smaller for the deuterated protein relative to those obtained for the protonated molecule, indicating that the I state shifts are more nativelike in the former case. To understand if this effect is the result of measurements on separate samples, reflecting perhaps the different labeling schemes (i.e.,

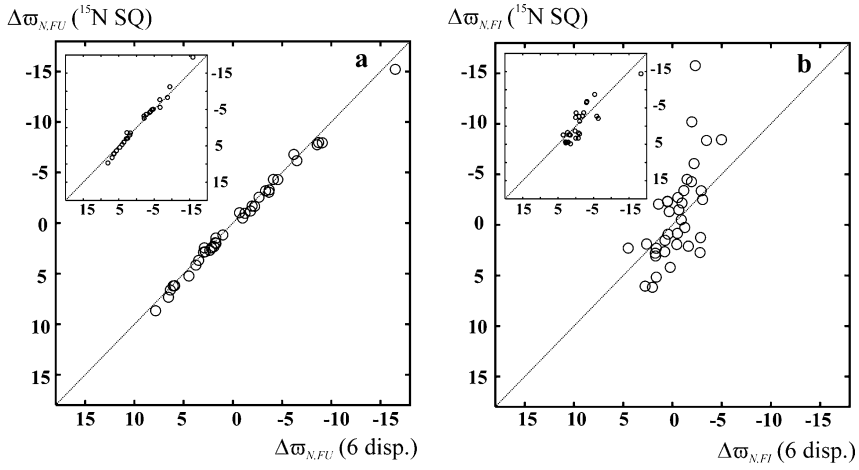

Figure 4. Comparison of chemical shift differences $\Delta\omega_{N,FU}$ (a) and $\Delta\omega_{N,FI}$ (b) obtained from the combined analysis of six types of dispersion data measured at 25 °C for deuterated Gly48Met Fyn SH3 (x axis) with the values obtained from an analysis of ^{15}N SQ data measured at five temperatures for protonated Gly48Met Fyn SH3[18] (y axis). Insets to the plots a and b, respectively, show a similar comparison (with the exception that ^{15}N SQ data is measured at three temperatures) for a subset of 26 residues of a partially deuterated Gly48Met Fyn SH3 domain (manuscript in preparation). ^{15}N SQ data were analyzed with the assumptions of (i) temperature dependence of the exchange rates governed by transition state theory and (ii) temperature-independent $\Delta\varpi_{N,FI}$ and $\Delta\varpi_{N,FU}$ values, as described elsewhere.[18]

^{1}H versus ^{2}H), we used an additional sample of ^{15}N/^{2}H Gly48Met Fyn SH3 for which the complete data set comprising the six types of ^{1}H−^{15}N dispersion profiles had been measured at three temperatures. This sample also included protonation at the Ile, Leu, Val methyl positions and at Phe and Trp for reasons that are not important to the present work (to be published). Two analyses have been performed on data obtained from this single sample, including one where the six dispersions at 25 °C were simultaneously fit (as for the perdeuterated protein) and a second where only the ^{15}N SQ profiles were analyzed, although all three temperatures were included (as for the fully protonated protein[18]). Simultaneous analysis of the six dispersion profiles (25 °C) produced values of $\Delta\varpi_{N,FI}$, $\Delta\varpi_{N,FU}$, $\Delta\varpi_{H,FI}$, and $\Delta\varpi_{H,FU}$ that are very close to those obtained in the present study of the perdeuterated construct. This emphasizes the robustness of the data and lends confidence in the extracted parameters obtained from the suite of six experiments. The insets to Figure 4a,b compare the ^{15}N chemical shift differences obtained from the analysis of the six dispersions at one temperature versus those generated from ^{15}N SQ data measured at three temperatures; it is clear that only a modest correlation in values of $\Delta\varpi_{N,FI}$ is produced from measurements on a single sample as well (inset to Figure 4b). This argues that the differences in $\Delta\varpi_{N,FI}$ values observed in Figure 4b (and its inset) are likely due to the assumptions made in the analysis of the ^{15}N SQ data and may also reflect the importance of recording a large number of dispersion data sets at a single set of conditions (temperature) for a robust estimate of chemical shift differences in the case of multisite exchange (see below).

Robustness of the Three-Site Solution Obtained Using Six Types of Dispersion Profiles. A concern in any multiple residue fit of dispersion data is that the results could be influenced by a few outlying residues that may not be reporting faithfully on the global process. To ascertain that this is not the case here, we have performed a series of jackknife simulations in which approximately 20% of the residues are removed randomly from the analysis to establish what influence (if any) individual residues have on the solution. In addition, Monte Carlo simulations have been performed to evaluate the effect of experimental uncertainties on the extracted exchange parameters (see Materials and Methods).

The mean values of the exchange rate constants $k_{ex,FI}$ and $k_{ex,FU}$ and populations p_I and p_U obtained in the jackknife simulations, where the dispersion data for a random subset of 10 out of 47 residues were excluded from the analysis, are in good agreement with the best-fit parameters obtained for all of the residues, with root-mean-squared deviations of these values somewhat higher than the uncertainties of the best-fit parameters, as estimated using the covariance matrix method[26] (Table 1). The chemical shift differences (Figure 5a) are also reproduced with reasonable accuracy, establishing that the combined fitting of six types of dispersion profiles per residue is robust with respect to selection of the residue set. Similar results are obtained in Monte Carlo simulations[26] (20 runs) where normally distributed random noise was added to exact synthetic dispersion data generated for 47 residues of Gly48Met Fyn SH3 using the best-fit parameters listed in Tables 1 and 2. Uncertainties of 2% were assumed for ^{1}H,^{15}N SQ, and ^{1}H,^{15}N MQ data and 4% for ^{1}H−^{15}N ZQ, DQ data. The target $k_{ex,FI}$, $k_{ex,FU}$, p_I, and p_U values were reproduced to within 20%, and the $\Delta\varpi_{N,FI}$, $\Delta\varpi_{N,FU}$, $\Delta\varpi_{H,FI}$, and $\Delta\varpi_{H,FU}$ values that were obtained are shown in Figure 5b. Not surprisingly, in both jackknife and Monte Carlo simulations, the parameters that describe the unfolded state U (5.13%) are obtained with better precision than the parameters of the low populated intermediate I (0.73%). Thus, for the vast majority of residues, root-mean-squared deviations of the chemical shift differences $\Delta\varpi_{H,FI}$ ($\Delta\varpi_{N,FI}$) are about 0.1 (0.5) ppm, 1 order

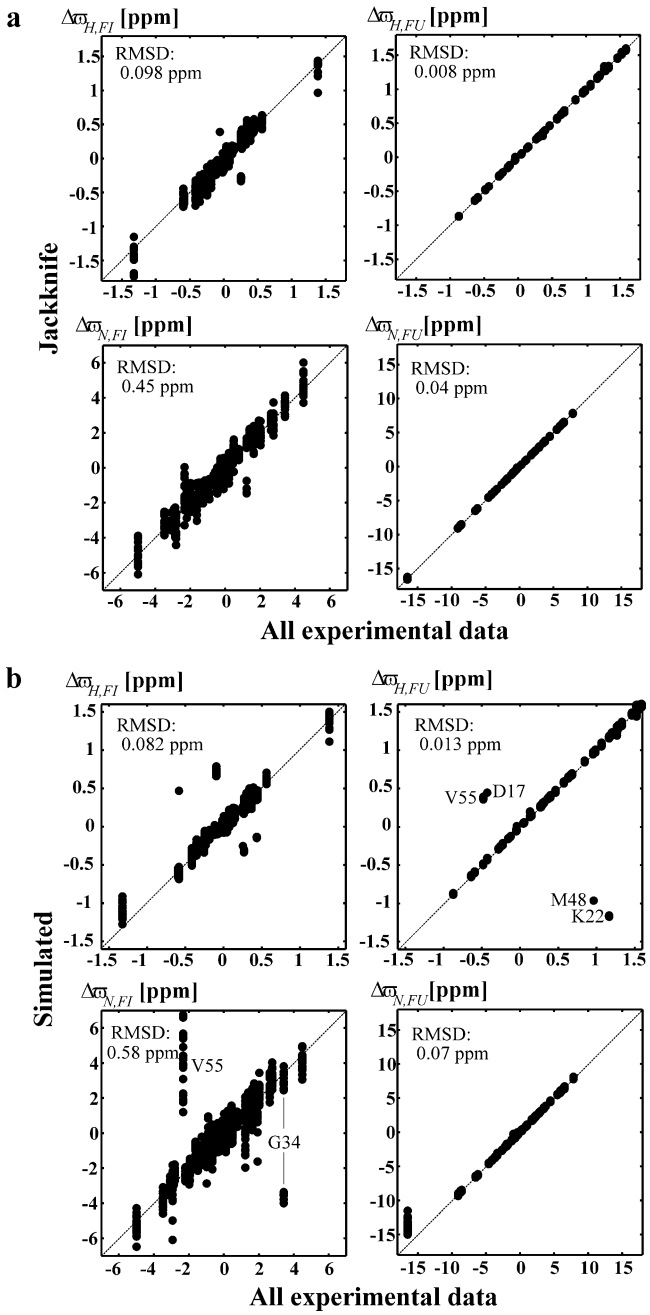

Figure 5. (a) Distributions of the chemical shift differences $\Delta\varpi_{H,FI}$, $\Delta\varpi_{H,FU}$, $\Delta\varpi_{N,FI}$, and $\Delta\varpi_{N,FU}$ from the solutions with the lowest "global" χ^2 values obtained using a jackknife simulation protocol (described in Materials and Methods) that was repeated 25 times, plotted as a function of the chemical shift differences obtained from the "global" fit of dispersion profiles using the full set of 47 residues (Table 2). (b) Distributions of the chemical shift differences from the solutions with the lowest "global" χ^2 values obtained in a Monte Carlo simulation that involved 20 separate computations (see Materials and Methods), as a function of the chemical shift differences from data fits of all 47 residues (Table 2). In a number of cases the signs of shift differences are inverted (see text) giving rise to anti-diagonals in the plots. These outliers were excluded from the calculation of the root-mean-squared deviations.

of magnitude higher than 0.01 ppm (0.1 ppm) obtained for $\Delta\varpi_{H,FU}$ ($\Delta\varpi_{N,FU}$) (see Figure 5a,b). Interestingly, $\Delta\varpi_{N,FI}$, $\Delta\varpi_{N,FU}$ are less well determined for Val55. For this residue, the exchange kinetics are in the slow regime ($\Delta\varpi_{N,FU} = -16.5$ ppm), and CPMG methods are not optimal for the extraction of parameters. In approximately half of the Monte Carlo simulations the sign of $\Delta\varpi_{N,FI}$ (along with the signs of $\Delta\varpi_{H,FI}$, $\Delta\varpi_{H,FU}$, and $\Delta\varpi_{N,FU}$) is inverted for Gly 34 (Figure 5b) and sign inversion occurs for residues Asp 17, Lys 22, and Met 48, reflecting the small values of $\Delta\varpi_{N,FU}$ for these residues (see section on spectral reconstruction).

Discrimination between Two- and Three-Site Exchange Models on a per-Residue Basis. In the Gly48Met Fyn SH3 domain, all residues participate in the same exchange process[18] (i.e., folding), so that the combined analysis of dispersion data for multiple sites is well-justified. In many cases of interest, however, exchange processes are local (i.e., involve only a few residues with significant ^{15}N and/or ^{1}H SQ dispersions). The uncertainties in experimental $R_{2,eff}$ rates (1 to 2% or more) are usually too high for the effective discrimination between two-site and three-site exchange on the basis of ^{15}N SQ dispersion data exclusively, if data from only a *single* amide group is considered. To establish whether reliable residue-specific parameters of three-site exchange can be extracted from the extended data set used in this work, we have performed an analysis involving the six dispersions for individual residues. To our surprise, the three-site exchange model produced superior fits of the data relative to a two-site scheme, $\chi^2_{2-site}/\chi^2_{3-site} > 1.09$ (corresponding to an F-test confidence of 99.9%), for only 14 residues with $|\Delta\varpi_{N,FU}| > 2.0$ ppm or $|\Delta\varpi_{H,FU}| > 0.2$ ppm (out of a total of 40). The ratio, $\chi^2_{2-site}/\chi^2_{3-site}$, was greater than 1.5 for only three residues (Trp37, Ile50, and Ser52). Numerical simulations show that the discrimination between two-site and three-site models of chemical exchange improves with increasing frequency separation between the low populated I and U states. Furthermore, for the exchange parameters of the ^{15}N/^{2}H Gly48Met Fyn SH3 domain (Table 2) the three-site exchange model provides no improvement in data fits with respect to the two-site model if $\Delta\varpi_{j,FI}/\Delta\varpi_{j,FU}$ is close to 1 for both ^{1}H and ^{15}N, irrespective of the values of $\Delta\varpi_{j,FI}$ and $\Delta\varpi_{j,FU}$. Finally, in simulations where $k_{ex,IU}$ values are varied, with other exchange parameters fixed, discrimination between two- and three-site exchange becomes increasingly difficult as $k_{ex,IU}$ becomes significantly smaller or larger than $\Delta\omega_{IU}$, as expected.

4. Concluding Remarks

The three-site folding of an ^{15}N-labeled deuterated Gly48Met mutant of the Fyn SH3 domain has been studied using a suite of six relaxation dispersion experiments that measure exchange contributions to spin relaxation of backbone amide ^{1}H and ^{15}N spins. The combined analysis of the dispersion curves exploits the fact that they report on the same set of physical parameters. In contrast to the quantification of three-site exchange by ^{15}N SQ measurements exclusively,[18] the analysis of six ^{1}H$-^{15}$N dispersion experiments does not require an extensive sampling of experimental conditions (e.g., temperature) nor does it depend on the set of assumptions that often accompanies such a sampling (e.g., some functional form for the temperature dependence of both exchange rates and chemical shift differences). The fits benefit significantly from the combined use of data measured for multiple residues, although in some cases robust three-site exchange parameters can be extracted for individual amide groups. Significantly, the experiments facilitate the extraction of the absolute signs of ^{1}H and ^{15}N chemical shift differences between exchanging sites and allow the near complete reconstruction of ^{1}H$-^{15}$N correlation maps for the invisible I ($p_I = 0.7\%$) and U ($p_U = 5\%$) states.

Acknowledgment. This work was supported by a grant from the Canadian Institutes of Health Research (CIHR) to L.E.K. D.M.K., P.N., and A.M. acknowledge postdoctoral support from the CIHR, the Deutsche Forschungsgemeinschaft (NE 1197/1-1), and the Natural Sciences and Engineering Research Council of Canada, respectively. L.E.K. holds a Canada Research Chair in Biochemistry.

Supporting Information Available: Three figures, similar to Figure 1, showing the six dispersion profiles of residues Glu11, Lys22, and Val58 and a summary of the theory involved in calculating dispersion profiles assuming either two- or three-site chemical exchange. This material is available free of charge via the Internet at http://pubs.acs.org.

JA054550E